Switching Strategies for DTC on Asymmetric Converters Driving Induction Motors

José A. Restrepo, José M. Aller, Julio C. Viola, Alexander Bueno, Víctor M. Guzmán, María I. Giménez; Universidad Simón Bolívar, Valle de Sartenejas, Baruta, Edo. Miranda; Caracas, Venezuela

Abstract

In this work, the possibilities offered by the additional switching states present in an asymmetric three phase converter (compared with the existing states in the conventional three phase inverter) are studied in order to improve the performance of Direct Torque Control induction motor drives. The proposed algorithms make use of these additional switching states sets in order to increase the operational range of the asymmetric converter and to reduce the ripple in the system variables. Simulated and experimental results obtained for different switching sets are presented and compared.

Introduction

Asymmetric converters are usually found in the power stage of highly non-linear machines such as stepper-motors and switch reluctance motors. Due to its structure these converters present more switching states than conventional inverters. However, few control strategies exploiting the presence of those additional states have been developed. A control scheme using the Direct Torque Control (DTC) philosophy was presented in [1-4] for the switched reluctance motor drives, where flux and torque are directly controlled through the stator voltage. The DTC technique can also be applied on induction motors driven by asymmetric converters, limiting flux and torque ripples to pre-calculated hysteresis bands. The DTC scheme has many advantages over conventional control techniques, such as a fast dynamic response, simplicity and robustness, but their disadvantages are variable power stage commutating frequency and inherent ripples in stator flux, current and generated motor torque.

For induction motors, the asymmetric converters are a possible solution to avoid operation faults due to short-circuits (in one or more phases) that can occur when conventional inverters are used to drive these kind of motors [5]. In this case is necessary to use an induction motor with independent stator windings in order to make a proper connection between the motor and the converter, as shown in Fig. 1. With this topology, as explained in the next section, there are 64 possible switching states, which produce 27 different control vectors instead of the 8 basic control vectors produced by the conventional inverter.

The most important characteristics of both converters types are summarized in Table I. In general terms the first three items are advantages of the asymmetric converter while the last three are advantages for the conventional inverter.

In this work, the capability of employing the previously unused asymmetric converter control vectors is investigated in order to perform improved DTC algorithms for induction motors with independent stator windings. Simulations, performed using an induction motor model in space vectors running in a Digital Signal Processor ADSP-21369 from Analog Devices, as well as experimental results, obtained using a test rig called "Plataforma III", developed by the Industrial Systems and Power Electronics Group (GSIEP) at Simón Bolívar University, are presented for several cases.

Asymmetric converter

Fig. 1 shows the diagram of the three phase asymmetric converter used in this work. Any converter with six independent and controlled switching devices, each of which can be ON or OFF (2 states) has $2^6 = 64$ possible switching states, however is very

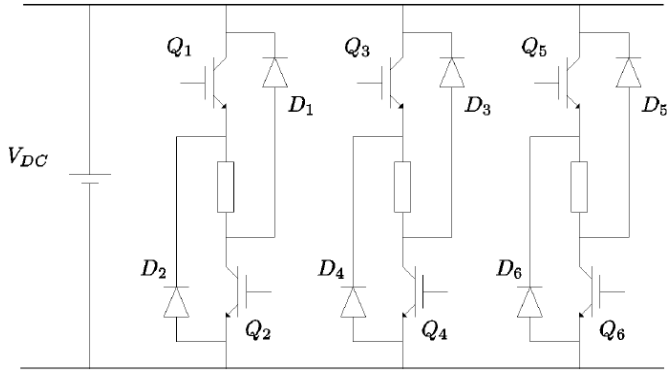

Fig. 1: Circuit diagram of the three phase asymmetric converter

Table I: Comparison between Asymmetric and Conventional Converters characteristics

	Characteristics	Asymmetric	Conventional
1	Switching states	27 possible switching states	8 switching states
2	Commutation failures	Non possible	Possible
3	Fault tolerant operation	Up to 2 faulty devices	Impossible
4	Current motor de-rating	Required due to unidirectional currents	No required
5	Machine windings	Open winding required	No special requirements
6	Device casing	Independent access to all terminals required	All cases acceptable

important to determine the validity of these states in order to define the number of valid space vectors for control purposes.

In the conventional three phase converter, 37 out of the 64 switching states are forbidden states due to short circuits of the DC link. There are only eight valid states that produce the corresponding space vectors, two of which correspond to space vector zero. The remaining 19 unused states have a corresponding valid state, so no additional space vectors can be obtained from these unused states.

In the asymmetric converter, all of the 64 possible states are valid states (do not produce operation faults due phase short circuits). These 64 switching states produce 27 valid voltage space vectors, that can be categorized in five different sets. To define these sets, it is necessary to analyze the possible states for each one of three branches of the asymmetric converter. Each branch has the following three possible states:

Branch state {1}: Obtained when both switches are turned on, therefore the motor phase is connected to the DC link.

Branch state {0}: Obtained when one switch is turned on and the other is turned off, therefore both terminals of the motor phase are connected to the same electrical point (upper or lower bar, through one active switch and one diode) if the current in the branch is larger than zero.

Branch state {– 1}: Obtained when both switches are turned off, therefore the motor phase is connected to the DC link with reverse polarity (through the diodes) if the current in the branch is larger than zero.

The combination of these three branch states for each one of the symmetrical converter branches produces the previously mentioned $3^3 = 27$ voltage space vectors.

Those voltage space vectors are obtained using the following expression:

$$\overrightarrow{v_s} = \sqrt{\frac{2}{3}} V_{DC} \left[1 \quad e^{j2\pi/3} \quad e^{j4\pi/3} \right] \cdot \left[S_{ph1} \quad S_{ph2} \quad S_{ph3} \right]^t \tag{1}$$

where S_{ph1}, S_{ph2}, S_{ph3} are the switching states of each branch.

Using (1), the obtained space vectors are shown in Fig. 2. These vectors can be classified in the following sets:

a) Three zero magnitude space vectors: {(– 1, – 1, – 1), (0, 0, 0), (1, 1, 1)

b) Six space vectors obtained with the combination of branch states {0} and {1}, including at least one {0} in each combination. This is the same set produced by the conventional inverter. Given these vectors magnitude when compared with the other vectors, this will be called the small positive space vectors set. The {0} vectors requires a branch current larger than zero, that will circulate through the diodes

c) Six space vectors obtained with one branch in {1}, other in {0} and the third one in {– 1}. This set will be called the medium space vectors set. The {0} and {1} vectors requires a branch current larger than zero, that will circulate through the diodes

d) Six space vectors obtained with the combination of {– 1} and {1} in each converter branch, without a zero state. This set will be called the large space vectors set.

e) Six space vectors obtained with the combination of branch states {0} and {– 1}, including at least one {0} in each combination. These vectors have the same magnitude that the positive small space vectors set, but requires a branch current larger than zero, that will circulate through the diodes. This set will be called the small recovery space vectors set.

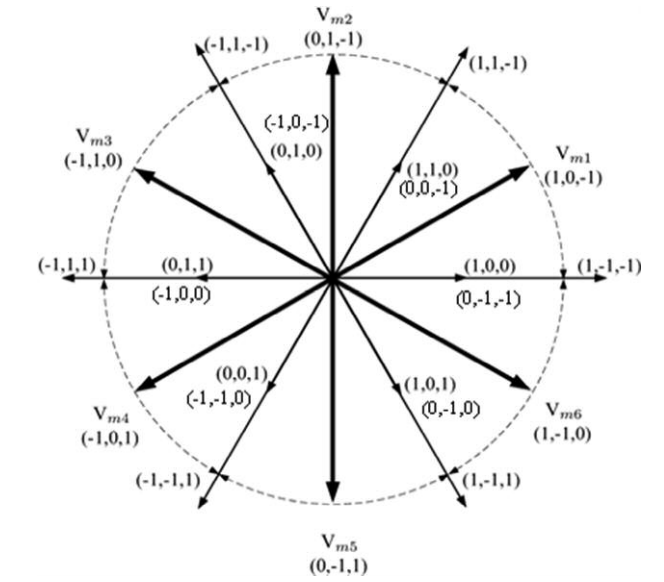

Fig. 2: Space vectors sets for the asymmetric converter

Table II: The state of the asymmetric converter switches for the medium space vector set

V_s	Q_1	Q_2	Q_3	Q_4	Q_5	Q_6
V_0	0	1	0	1	0	1
V_{m1}	1	1	0	1	0	0
V_{m2}	0	1	1	1	0	0
V_{m3}	0	0	1	1	0	1
V_{m4}	0	0	0	1	1	1
V_{m5}	0	0	0	0	1	1
V_{m6}	1	1	0	0	0	1
V_{m7}	1	1	1	1	1	1
1 = ON			0 = OFF			

As an example, Table II shows the state of each switch when the medium space vectors set is applied.

DTC algorithm

The conventional DTC algorithm was proposed by Takahashi et al. [6], uses a calculator block to obtain the computed values for the instantaneous stator flux and electric torque in the machine. The calculated torque and flux values are compared with the corresponding reference values and their error signals are fed to hysteresis comparators. The output of these comparators, together with the information of the angular flux location, are used to address the switching table. In [6], the stator flux space vector plane is divided in six regions and Table II shows the corresponding look-up table for the classical DTC algorithm. The stator flux linkage can be derived by integrating the electromotive force in the stator winding using the following expression.

$$\vec{\Psi}_s = \int \left(\vec{v}_s - R_s \vec{i}_s \right) dt \tag{2}$$

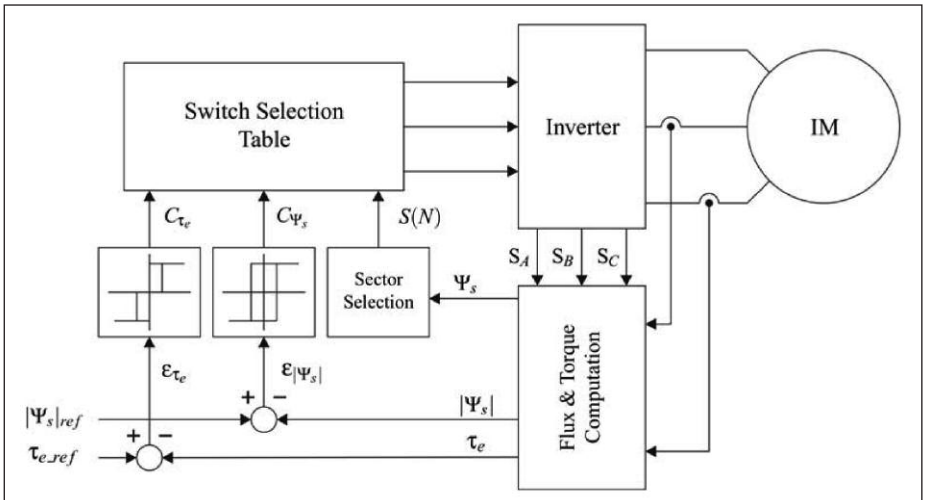

Fig. 3: Block diagram of the classical direct torque controller

$$\begin{cases} \left[\vec{v}\right] = \left[R\right]\left[\vec{i}\right] + \left[L\right]p\left[\vec{i}\right] - j\omega\left[\tau\right]\left[\vec{i}\right] \\ M_{sr}\Im m\left\{\vec{i}_s \cdot \left(\vec{i}_r^{\,s}\right)^*\right\} = J\dot{\omega} \end{cases} \quad (4)$$

where

$$\left[\vec{v}\right] = \begin{bmatrix} \vec{v}_s \\ \vec{v}_r^{\,s} \end{bmatrix}; \left[\vec{i}\right] = \begin{bmatrix} \vec{i}_s \\ \vec{i}_r^{\,s} \end{bmatrix}; \left[R\right] = \begin{bmatrix} R_s & 0 \\ 0 & R_r \end{bmatrix};$$

$$\left[L\right] = \begin{bmatrix} L_s & M_{sr} \\ M_{sr} & L_r \end{bmatrix}; \left[\tau\right] = \begin{bmatrix} 0 & 0 \\ M_{sr} & L_r \end{bmatrix}$$

$$\vec{x} = \sqrt{2/3}\left[x_a + e^{j\frac{2\pi}{3}}x_b + e^{j\frac{4\pi}{3}}x_c\right];$$

$$\vec{x}^{\,s} = \vec{x} \cdot e^{-j\theta}\ ;\ \dot{\theta} = \omega$$

Table III: DTC space vector selection

$\varepsilon_{\tau g}$	$\varepsilon_{\psi s}$	S(1)	S(2)	S(3)	S(4)	S(5)	S(6)
– 1	– 1	$\vec{v}_5$	$\vec{v}_6$	$\vec{v}_1$	$\vec{v}_2$	$\vec{v}_3$	$\vec{v}_4$
0	– 1	$\vec{v}_0$	$\vec{v}_7$	$\vec{v}_0$	$\vec{v}_7$	$\vec{v}_0$	$\vec{v}_7$
1	– 1	$\vec{v}_3$	$\vec{v}_4$	$\vec{v}_5$	$\vec{v}_6$	$\vec{v}_1$	$\vec{v}_2$
– 1	1	$\vec{v}_6$	$\vec{v}_1$	$\vec{v}_2$	$\vec{v}_3$	$\vec{v}_4$	$\vec{v}_5$
0	1	$\vec{v}_7$	$\vec{v}_0$	$\vec{v}_7$	$\vec{v}_0$	$\vec{v}_7$	$\vec{v}_0$
1	1	$\vec{v}_2$	$\vec{v}_3$	$\vec{v}_4$	$\vec{v}_5$	$\vec{v}_6$	$\vec{v}_1$

The electric torque is obtained multiplying the stator flux linkage and the stator current space vectors.

$$\tau_e = \vec{\Psi}_s \times \vec{i}_s \quad (3)$$

The electric torque and the stator linkage flux are adjusted by the DTC algorithm applying the stator voltage space vector that compensates both errors. In the case of the conventional converter there are only five possible stator voltage space vectors available in each region for the compensation. In the asymmetric converter there are many more available choices. The optimum switching table for equal size space vectors with π/3 phase lag between them, used in the classical DTC algorithm, can still be applied in this general case.

The block diagram for the classical DTC algorithm is shown in Fig. 3 and the same control block can be used together with Table III with the asymmetric converter, but the sector selection will depend on the set of vectors used for the implementation of the algorithm.

In the following sections, simulations and experimental results for several cases are presented.

Simulated and experimental results

For the simulations, the induction machine was modelled in the stator coordinates frame using the following equations.

The system was simulated by programming the induction machine equations and the DTC vector selection algorithms using C language, running on an Analog Devices digital signal processor (ADSP-21369) [7]. The differential equations modelling the induction machine were solved by using a standard fixed step fourth order Runge-Kutta Ordinary Differential Equations (ODE) integrator, the integration step was 10 μs. The simulations are simplified by using a fixed voltage DC link; the electrical parameters for the induction machine are given in Table IV.

For the experimental part, the DTC algorithms were implemented on a custom build floating point DSP based test-rig (ADSP-21369 at 320 MHz), developed by the Industrial Systems and Power Electronics Group (GSIEP) at Simón Bolívar University [8]. The power stage uses six 27A, 600V, IGBTs with one 2200 μF 450 V capacitor in the DC link. The switching signals where synthesized with an on-chip PWM operating at 10 kHz. The sampling frequency was synchronized with the beginning of the control cycle. Fig. 4 shows the actual test rig used for the simulation and experimental tests.

Simulation and experimental results are presented including space vector flux, phase 'a' current and electric torque for each study case. In all cases the flux reference is 0.7 Wb.

Application of the small positive state vectors set

The first experiments were done applying the small positive space vectors set in order to analyze the system performance when the asymmetrical converter is used to drive an induction motor with this vector set [9].

Controlling the asymmetric converter, using the positive small vectors or the negative small vectors alone, will require the adjustment of the zero sequence component in the stator voltages for proper operation. For the small positive vectors, a negative value of the zero sequence component is required to reduce the DC component in the stator currents, while for the small recovery vectors a positive value of the zero sequence component will be required to provide enough current to produce the regenerative vectors.

Table IV: Electrical parameters for the induction machine

Model	P_n	V_n	I_n	n_n	f_n	R_s	R_r	L_s	L_r	M_{sr}
SKI80-43	1 HP	220/380 V	3.3/1.92 A	1400 rpm	50 Hz	8.2 Ω	10.6 Ω	0.866 H	0.866 H	0.083 H

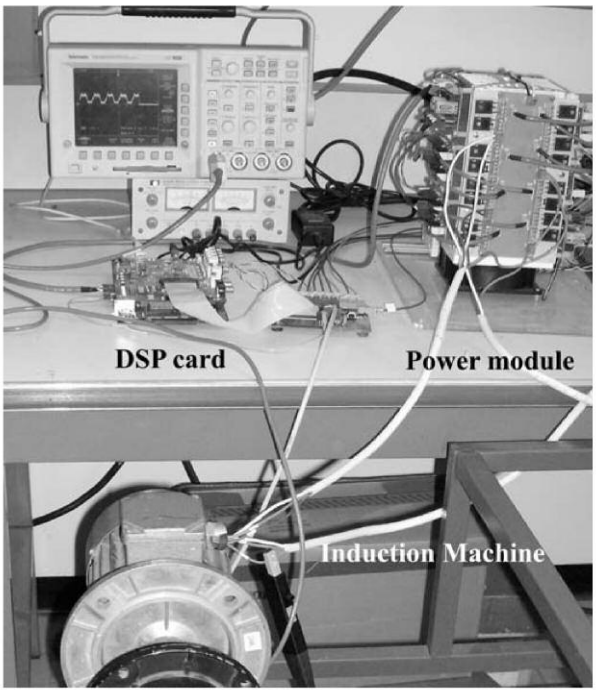

Fig. 4: Test rig used for the simulation and experimental tests

Fig. 5 shows the simulation results and Fig. 6 the experimental results for the small positive space vectors set. The results show that the flux is maintained within the selected hysteresis band, and the current and torque have the typical ripple present in DTC algorithms. These results prove the capacity of the asymmetric converter to produce a circular flux vector as shown in Fig. 5a and Fig. 6a, using unidirectional phase current presented in Figs. 6b and 6b. By comparing Figs. 5c and 6c it can be concluded that the simulated and experimental electric torque ripple obtained using this vectors set are similar. The observed differences could be easily explained by model simplifications. These results prove that the asymmetric converter can be successfully applied on induction motor drives when a tolerant fault system is required. However, this configuration requires a bias DC current which increases the rms current, the cooper losses and reduces the rated power.

Application of the small recovery state vectors set

The next step is to test the small recovery space vectors performance [10]. As said before, controlling the asymmetric converter using the small recovery space vectors alone, will require the adjustment of the zero sequence component in the stator voltages for proper operation. A positive value of the zero sequence component will be required to provide enough current to produce the regenerative vectors.

Fig. 7 shows the simulation results and Fig. 8 the experimental results for the small recovery space vectors set. As in the previous case, the results show that the flux is maintained within the selected hysteresis band. The current and torque have the typical ripple present in DTC algorithms and the asymmetric converter produces a rotating field as shown in Fig. 7a and Fig. 8a, using unidirectional phase current as in Figs. 7b and 8b. Figs. 7c and 8c show that experimental electric torque ripple is smaller than the simulated one. Summing up, there are not significant differences between positive and recovery vectors set behaviour when controlling an asymmetric converter for driving an induction motor.

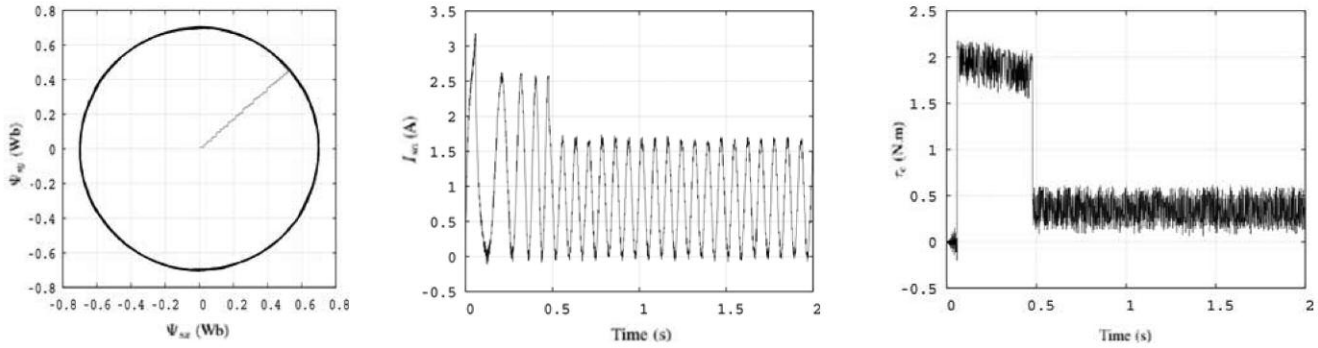

(a) Stator flux (b) Phase ‘a’ current (c) Electric torque

Fig. 5: Simulation results for the DTC with small positive space vectors set

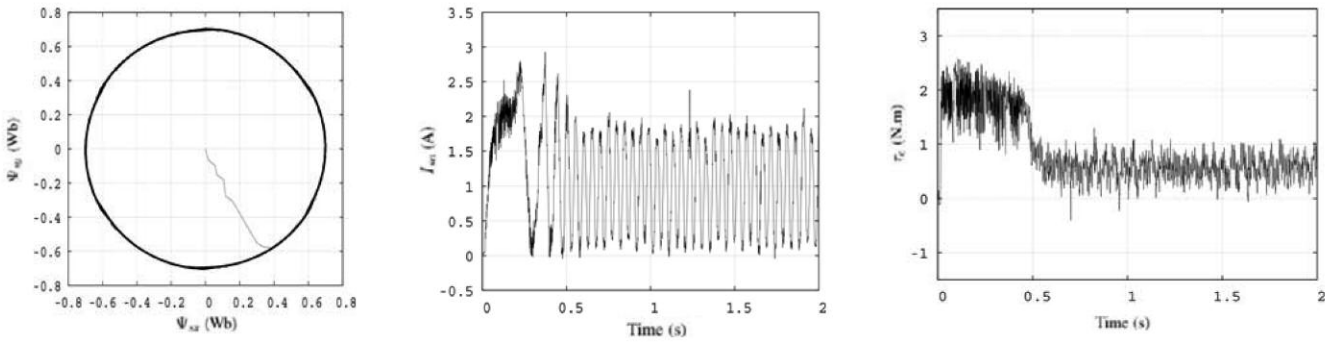

(a) Stator flux (b) Phase ‘a’ current (c) Electric torque

Fig. 6: Experimental results for the DTC with small positive space vectors set

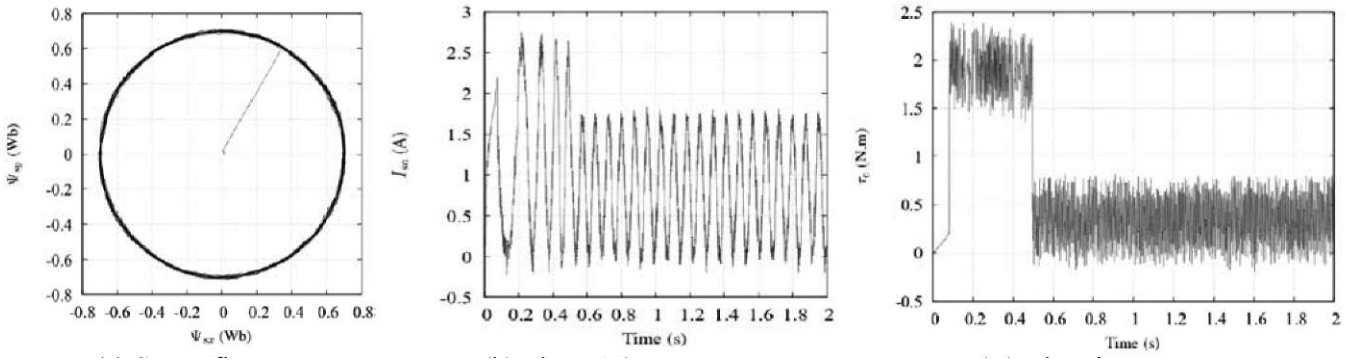

(a) Stator flux (b) Phase 'a' current (c) Electric torque

Fig. 7: Simulation results for the DTC with small recovery space vectors set

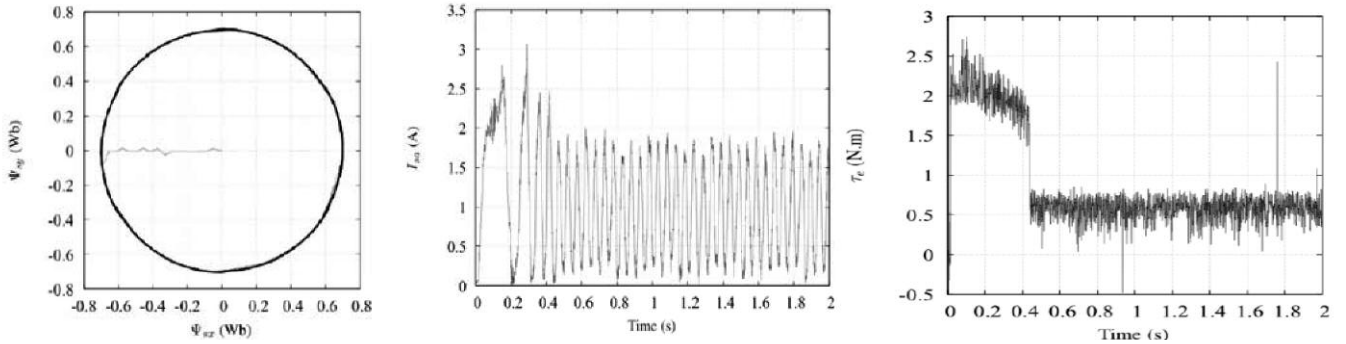

(a) Stator flux (b) Phase 'a' current (c) Electric torque

Fig. 8: Experimental results for the DTC with small recovery space vectors set

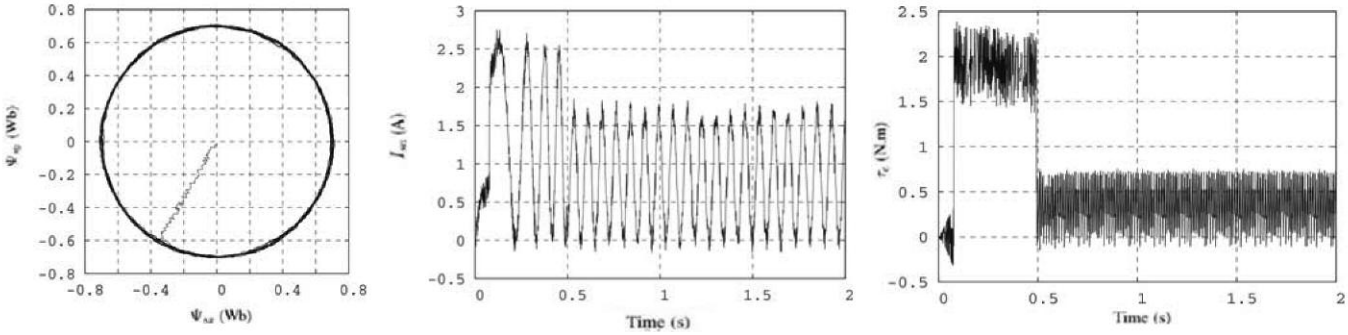

(a) Stator flux (b) Phase 'a' current (c) Electric torque

Fig. 9: Simulations for the DTC with medium size space vectors set

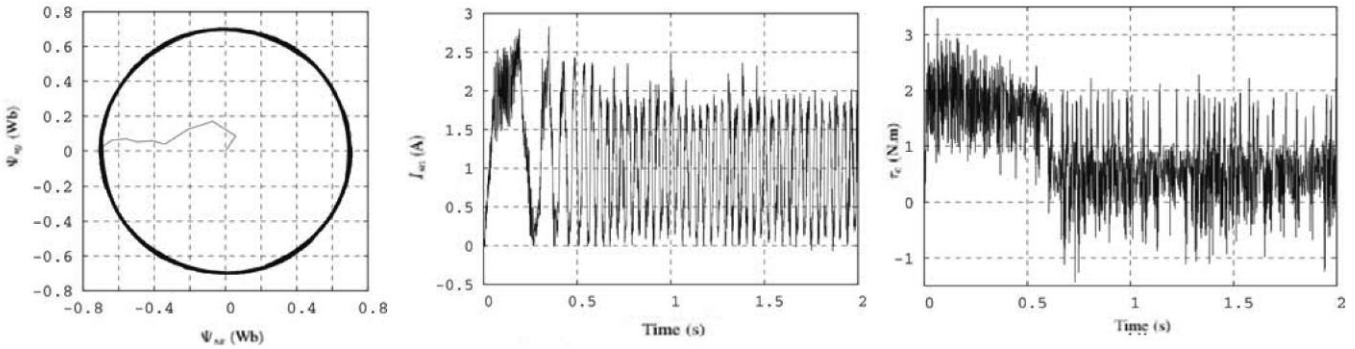

(a) Stator flux (b) Phase 'a' current (c) Electric torque

Fig. 10: Experimental results for the DTC with medium size space vectors set

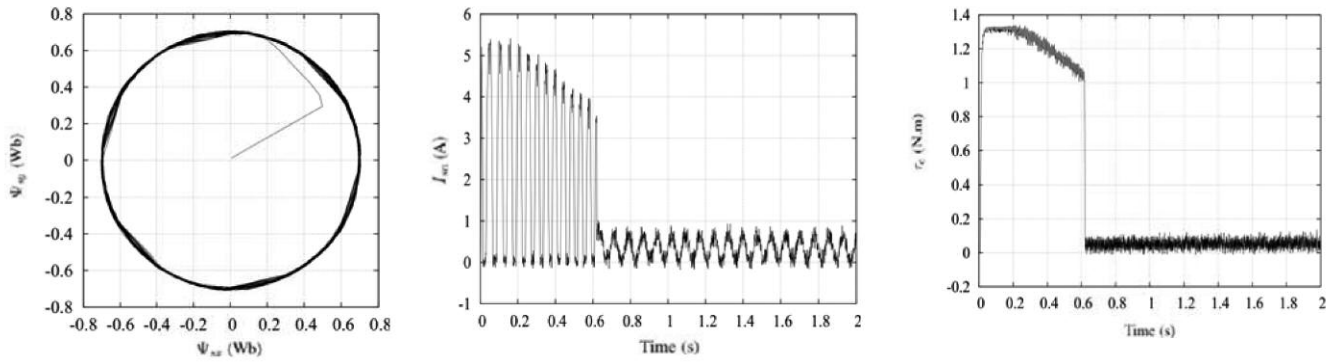

(a) Stator flux (b) Phase 'a' current (c) Electric torque

Fig. 11: Simulations for the proposed combination of small positive and recovery space vectors sets

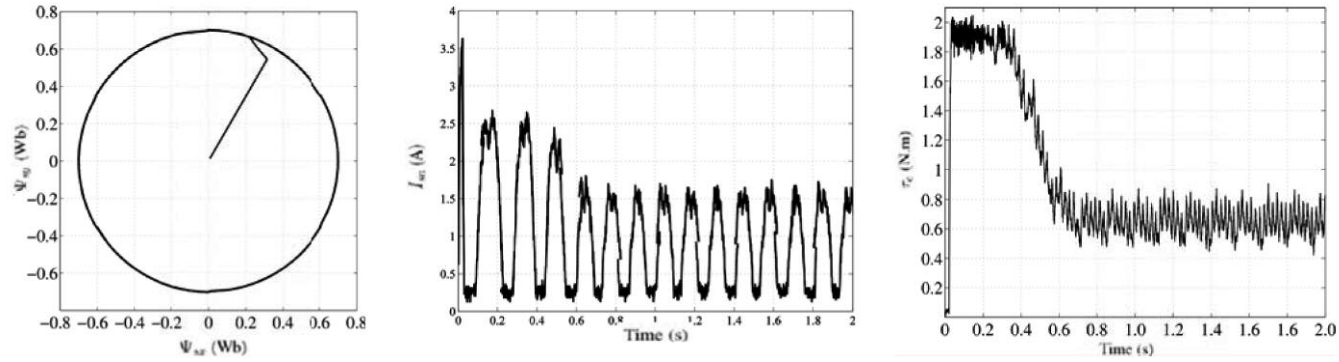

(a) Stator flux (b) Phase 'a' current (c) Electric torque

Fig. 12: Experimental results for the proposed combination of small positive and recovery space vectors sets

Application of the medium space vectors set

The work with the medium space vectors set was reported initially in [11]. Figure 9 shows the simulation results and Fig. 10 the experimental results for the medium space vectors set. In this case, an additional control loop is added to the system to limit the phase currents magnitude. This is achieved by reducing the voltage space vector if the current is large. As before, the results show that the flux is maintained within the selected hysteresis band, the current and torque have the typical ripple present in DTC algorithms and the asymmetric converter produces a rotating field as shown in Figs. 9a and 10a, using unidirectional phase current presented in Figs. 9b and 10b. Figures 9c and 10c show that the experimental electric torque ripple is bigger than the simulated one because the larger vectors size affects the induction motor saturation. Finally, with the medium vectors set, the DC link voltage is better utilized allowing higher speeds and a better dynamic response.

Combination of the small positive and recovery space vectors sets

A new DTC strategy was tested combining the positive and recovery small vectors set [12]. In the proposed algorithm the main idea is to guarantee enough energy in the phase leakage inductances to maintain the regenerative states when a state is required. To attain this, the algorithm tries to use the negative set of vectors whenever is possible, and the positive set of vectors if the conditions are not appropriate for the former. So, if the current in any phase falls below a pre-selected minimum value, the algorithm will synthesize the required voltage space vector with the positive set, otherwise it will use the negative set.

The experimental results for the combination of small positive and recovery space vectors sets are shown in Figs. 11 and 12. In Figs. 11b and 12b the phase current is kept positive by switching between the two sets of small voltage space vectors, and this control action provides enough zero sequence current component in the stator windings without the need to add any additional component to the phase voltages. Figs. 11a and 12a show the evolution of the stator flux, following a circular trajectory similar to the one obtained with all the other space vectors sets. Figs. 11c and 12c show the electric torque, where it is possible to observe the significant ripple reduction when this strategy is applied. This combination gives the lowest ripple torque of the all tested strategies for both simulated and experimental results.

Fig. 13 presents steady state currents oscillogram for the three phases. As can be seen, the currents have always positive values with the corresponding phase shift. The combination of the three DC components produces a null flux in the machine airgap.

Conclusions

All the previous results show that the asymmetric converter can be successfully applied on induction motor drives when a fault tolerant system is required using any of the possible state voltage vectors sets available for this converter configuration. Single space vectors sets require a bias DC current, which increases the rms current, the cooper losses and reduces the rated power losses.

However, when different space vectors sets are used together, as in the combination of the small positive and recovery space vectors sets, additional states can be used to add more entries to the switching table. A reduction of the current and torque ripple is obtained with the use of the additional states because this control

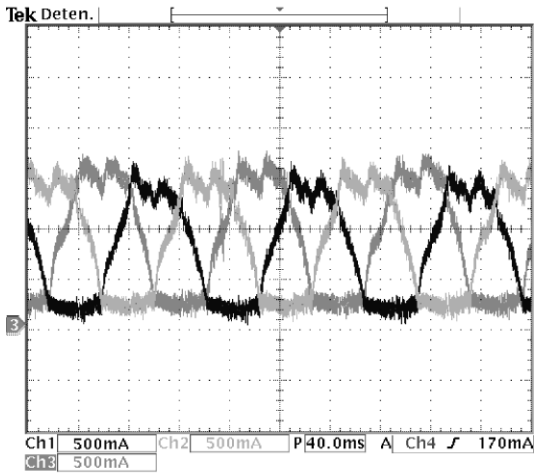

Fig. 13: Oscillogram of the three phase currents

action provides enough zero current component in the stator windings without the need to add any additional component to the phase voltages.

References

[1] A.D. Cheok and P.H. Hoon: A New Torque Control Method for Switched Reluctance Motor Drives, in 26th Anual conference of the IEEE Industrial Electronics Society, IECON 2000, Oct. 2000, pp. 387–392.

[2] A.D. Cheok and Y. Fukuda: A New Torque and Flux Control Method for Switched Reluctance Motor Drives, IEEE Trans. Power Electron., vol. 17, no. 4, pp. 543–557, Jul. 2002.

[3] R. Jeyabharath, P. Veena, and M. Rajaram: A Novel DTC Strategy of Torque and Flux Control for Switched Reluctance Motor Drive, International Conference on Power Electronics, Drives and Energy Systems, PEDES 06, Dec. 2006, pp. 1–5.

[4] H.J. Guo: Considerations of Direct Torque Control for Switched Reluctance Motors, in Proceedings of the 2006 IEEE International Symposium on Industrial Electronics, ISIE 2006, Jul. 2006, pp. 2321–2325.

[5] B. Welchko, T. Lipo, T.M. Jahns, S.E. Schulz: Fault Tolerant Three-Phase AC Motor Drive Topologies: A Comparison of features, Cost, and Limitations, IEEE Trans. on Power Electronics, Vol. 9, No 4, pp. 1108-1116, July 2004.

[6] I. Takahashi and T. Noguchi: A New Quick-Response and High-Efficiency Control Strategy of an Induction Motor, IEEE Trans. Ind. Appl., vol. IA-22, pp. 820–827, Sep./Oct. 1986.

[7] VisualDSP++ 4.5, C/C++ Compiler and Library, Manual for ADSP-21xxx DSPs, Analog Devices Inc, 2006.

[8] M.I. Giménez, V.M. Guzmán, J.A. Restrepo, J.M. Aller, J.C. Viola, A. Bueno: PLATAFORMA: A Useful Tool for High Level Education, Research and Development. Proceedings of the 7th International Caribbean Conference on Devices, Circuits and Systems, ICCDCS 2008, CD. ISBN 978-1-4244-1957-9 Pag. 1-6, 2008.

[9] A. Cabello, J.A. Restrepo, V.M. Guzmán, M.I. Giménez, J. Lara, J.M. Aller: Control Directo de Par del Motor de Inducción Usando un Convertidor Puente Asimétrico. Memorias del Seminario Anual de Automática, Electrónica Industrial e Instrumentación, SAAEI 2007, CD. pp. 177 – 181, Sept. 2007.

[10] J.A. Restrepo, M.I. Giménez, V. M. Guzmán, J.M. Aller, J.C. Viola: Aplicación del Conjunto de Vectores de "Recuperación" al Esquema de Control Directo de Par para el Motor de Inducción usando un Convertidor Puente Asimétrico. Memorias del Seminario Anual de Automática, Electrónica Industrial e Instrumentación, SAAEI 2008, CD. pp. C62.1 - C62.6, Sept. 2008

[11] A. Cabello, J.A. Restrepo, V.M. Guzmán, M.I. Giménez, J. Lara, J.M. Aller, A. Bueno: Uso del Conjunto de Vectores Espaciales de Amplitud Media Generado por un Puente Conversor Asimétrico Tolerante a Fallas para el Control Directo de Par de Motores de Inducción, Revista de Ingeniería de la UCV, Vol. 21, pp. 39-46, 2009.

[12] J.A. Restrepo, J.M. Aller, V.M. Guzmán, M.I. Giménez, J.C. Viola: Switching Strategies for DTC on Asymmetric Converters, 13th European Conference on Power Electronics Applications, EPE 2009, CD, pp P1-P9.

The authors

Jose Alex Restrepo was born in Cali, Colombia, in 1964. He received the Electronic Engineer degree and the M.Sc. in Electronic Engineering degree from the Universidad Simón Bolívar, Caracas, Venezuela, in 1988 and 1991, respectively, and the Ph.D. degree from the University of Manchester Institute of Science and Technology (UMIST), Manchester, U.K., in 1996. He is currently a Full Professor of electronics engineering with the Departamento de Electrónica y Circuitos, Universidad Simón Bolívar. In 2002, he was a Visiting Professor with the School of Electrical and Computer Engineering, Georgia Institute of Technology, Atlanta. His research interests include advanced control of electrical machines, artificial intelligence, power quality and digital signal processors applied to motion control.

Jose Manuel Aller was born in Caracas, Venezuela, in 1958. He received the Electrical Engineer degree from the Universidad Simón Bolívar, Caracas, in 1980, the M.Sc. in Electrical Engineering degree from the Universidad Central de Venezuela, Caracas, in 1982, and the Dr. in Industrial Engineering degree from the Universidad Politécnica de Madrid, Madrid, Spain, in 1993. He has been a Lecturer at the Universidad Simón Bolívar for 30 years, where he is currently a Full Time Professor in the Departamento de Conversión y Transporte de Energía teaching electrical machines and power electronics. He was the General Secretary of the Universidad Simón Bolívar from 2001 to 2005. He has been visiting professor at the Georgia Institute of Technology, Atlanta, USA, in 2000 and 2007. His research interests include space-vector applications, electrical machine control, power electronics and monitoring of electrical machines.

Alexander Bueno was born in Caracas, Venezuela in 1971. He received the Electrical Engineer degree and the M.Sc. in Electrical Engineering degree from the Universidad Simón Bolívar, Caracas, Venezuela, in 1993 and 1997, respectively. He has been a Lecturer at the Universidad Simón Bolívar for 16 years, where he is currently a Full Time Professor in the Departamento de Conversión y Transporte de Energía teaching electrical machines and power electronics. Currently, his research interests include space vector control applications, electrical machines, neural network estimators and power electronics.

Julio César Viola was born in La Paz (E.R.), Argentina, in 1975. He received the Electronics Engineer degree from the Universidad Tecnológica Nacional, Paraná (E.R.), Argentina, in 2000, and the Ph.D. degree from Universidad Simón Bolívar, Caracas, Venezuela, in 2008. In 2005, he joined the faculty of Universidad Simón Bolívar, Caracas,

Venezuela, as an Assistant Professor of Electronics Engineering. He became an Associate Professor in 2008. His current research interests include adaptive control of electrical machines using DSP and field-programmable gate array (FPGA), active power filters, and artificial intelligence.

Víctor Manuel Guzmán was born in Zaragoza, Spain, in 1952. He received the Electronic Engineer degree from the Universidad Simón Bolívar, Caracas, Venezuela, in 1975, and the M.Sc. and Ph.D. degrees in Power Electronics and Systems from the University of Manchester Institute of Science and Technology (UMIST), Manchester, U.K, in 1978 and 1991, respectively. He started working at the Department of Electronics and Circuits, Universidad Simón Bolívar in 1975, and since 1993 he has been a Full Professor in the mentioned Department. His research interests include power electronics circuit design, device modeling, and renewable energy sources.

María Isabel Giménez was born in Caracas, Venezuela, in 1952. She received the Electronic Engineer degree from the Universidad Simón Bolívar, Caracas, Venezuela, in 1974, and the M.Sc. and Ph.D. degrees in Power Electronics and Systems from the University of Manchester Institute of Science and Technology (UMIST), Manchester, U.K, in 1978 and 1991, respectively. She started working at the Department of Electronics and Circuits, Universidad Simón Bolívar in 1974, and since 1992 she has been a Full Professor in the mentioned Department. Her research interests include circuit simulations, modulation algorithms and power electronics system design.